Experimental study of the dynamics of $D + H_2$ reactive and inelastic collisions below 1.0 eV relative energy

David L. Phillips, Harold B. Levene, and James J. Valentini
Department of Chemistry, University of California, Irvine, California 92717

(Received 7 September 1988, accepted 20 October 1988)

We report the results of state-to-state dynamics experiments on the $D + H_2 \rightarrow HD + H$ reaction as well as $D + H_2 \rightarrow H_2^\dagger + D$ energy transfer at relative energies of 0.67 and 0.79 eV. Both product state distributions and absolute partial cross sections have been determined, from coherent anti-Stokes Raman scattering (CARS) spectra of the HD and $H_2^\dagger$ products recorded under single-collision conditions following pulsed-laser photolysis of DI to generate the D atom reactant. At both energies and for both reactive and inelastic collisions there is a strong dynamical bias against rotational and vibrational excitation of the product. However, at 0.67 eV there is an enhancement of both the relative and absolute yield of HD ($v' = 1$), and to a lesser extent $H_2(v' = 1)$, the only energetically accessible vibrationally excited product states. This may be the result of a Feshbach resonance at $\approx$0.65 eV, just above the $v' = 1$ threshold energy. Product quantum state distributions from quasiclassical trajectory calculations are in fairly good agreement with the experimental results, except that they do not show the $v' = 1$ enhancement at 0.67 eV. However, the partial cross sections from the trajectory calculations are systematically larger than those measured.

I. INTRODUCTION

As the simplest chemical reaction, the hydrogen exchange reaction holds a unique position in chemical dynamics, particularly theoretical chemical dynamics. It has been a testing ground for classical, semiclassical, and approximate quantum mechanical dynamical calculations,[1–6] and is one of only a few systems for which exact three-dimensional quantum mechanical calculations of the dynamics have been carried out.[7–14] The lightness of the nuclei in the hydrogen exchange reaction makes quantum effects such as tunneling[15–21] and dynamical resonances[9–13,22–25] important and observable.

Because of its significance we have chosen to carry out an extensive series of experimental studies on the hydrogen exchange reaction. Originally our experiments[26–31] focused on the $H + D_2 \rightarrow HD + D$ isotopic variant of the reaction and the associated rotationally and vibrationally inelastic collision process $H + D_2 \rightarrow D_2^\dagger + H$, at energies quite far above threshold, $\geqslant$1.0 eV, for which many product states are energetically accessible. More recently our experiments have involved the classic $H + H_2 \rightarrow H_2 + H$ isotopic variant at collision energies between 0.7 and 1.0 eV, where a rich spectrum of dynamical resonances is observed.[24,25] This publication deals with the remaining easily accessible isotopic variant of the reaction, $D + H_2 \rightarrow HD + H$, and the associated $D + H_2 \rightarrow H_2^\dagger + D$ inelastic collisions.

These $D + H_2$ collisions afford the only opportunity in our experiments to access collision energies not much greater than the reaction threshold. In our $H + D_2$ experiments collision energies below 0.76 eV are not accessible and for $H + H_2$ energies below 0.63 eV are not accessible, while for $D + H_2$ we can get lower than 0.48 eV. These restrictions are kinematic ones associated with the source of the reactant atom in our experiments, photolysis of HI(DI). We cannot produce H or D atoms with lab energies below about 1.0 eV by photolysis of HI or DI, due to limitations imposed by the electronic absorption spectrum of HI(DI). No other photolytic source can yield monoenergetic or nearly monoenergetic H(D) atoms with lab energies this low, so the limitations imposed by the HI(DI) photochemistry are absolute ones. The relative energy in the hydrogen exchange reaction using fast, photolytic hydrogen atoms and a thermal sample of hydrogen molecules is given approximately by

$$E_{\rm rel} = (\mu/m_{\rm atom})E_{\rm atom}, \tag{1}$$

where μ is the reduced mass of the atom + diatom collision pair, $m_{\rm atom}$ is the mass of the H(D) atom, and $E_{\rm atom}$ is the translational energy of the atom in the laboratory frame. The ratio $\mu/m_{\rm atom}$ is 0.8 for $H + D_2$, 0.67 for $H + H_2$, and 0.5 for $D + H_2$, and the 1.0 eV lower limit on $E_{\rm atom}$ imposed by the electronic absorption spectrum of HI(DI) yields the lower limits on $E_{\rm rel}$ for these reactions.

We describe here results of experimental studies of the $D + H_2$ reaction at $E_{\rm rel} = 0.67$ and 0.79 eV. These energies are not the lowest possible; exploration of the $D + H_2$ reaction dynamics near threshold will be done in subsequent experiments. The choice of these collision energies was influenced by the results of our recent $H + H_2$ state-to-state dynamics experiments, which reveal pronounced dynamical resonances, Feshbach resonances, at several relative energies, including 0.70 eV.[24,25] Resonances are often associated with energetic thresholds for particular product vibrational states. In the $H + H_2$ and $D + H_2$ reactions the $v' = 1$ thresholds are at collision energies of 0.66 and 0.61 eV respectively [for H_2 ($v = 0, j = 0$) reactant]. The opportunity to compare the state-to-state dynamics of $D + H_2 \rightarrow HD + H$ and $H + H_2 \rightarrow H_2 + H$ in the vicinity of a dynamical resonance seems particularly appealing. In fact, we do find evidence of a Feshbach resonance in $D + H_2 \rightarrow HD + H$ as well.

Even if resonance effects were absent, these lower collision energy $D + H_2$ experiments would be desirable as an

 0021-9606/89/031600-10$02.10

extension of our previous $E_{rel} \geqslant 1.0$ eV H + D_2 studies.[26–31] These H + D_2 experiments at collision energies of 0.98, 1.10, and 1.30 eV yielded product state distributions and partial cross sections that are in surprisingly good agreement with the results of quasiclassical trajectory calculations (QCT).[26–33] Will this agreement between experiment and QCT calculations extend to lower collision energies and other isotopic combinations of the hydrogen exchange reaction? Since we observe what appear to be dynamical resonance effects in D + $H_2 \rightarrow$ HD + H at $E_{rel} = 0.67$ eV the quasiclassical trajectory calculations should not provide a good description of the dynamics at this energy. In fact, there is reasonable agreement between the QCT calculations and experiment for the relative population distributions at 0.79 eV, while at 0.67 eV where the resonance effect appears, the QCT-experiment agreement is not so good, particularly for the ratio of $v' = 1$ to $v' = 0$. Overall the QCT calculations do not give as good agreement with experiment as they did for H + D_2 at higher collision energies.

In the next section we give a brief description of the experimental apparatus and method used to do these experiments, while Sec. III presents the results of the experiments. In Sec. IV we compare these experimental results with results of QCT calculations, with our results from experiments with other isotopic variants of the hydrogen exchange reaction, and with the results of crossed molecular beam experiments of D + $H_2 \rightarrow$ HD + H at relative energies between 0.85 and 1.20 eV.[34,35] Our conclusions about the dynamics of D + H_2 collisions are summarized in Sec. V.

II. EXPERIMENT

As in our previous H + D_2 and H + H_2 state-to-state dynamics experiments we use coherent anti-Stokes Raman scattering (CARS) spectroscopy to measure the rotational and vibrational state distributions of the reactive HD and inelastic H_2 products of D + H_2 collisions under single-collision conditions. The D atoms are generated by pulsed-laser photolysis of DI. Since the experimental apparatus and methodology used here have been described extensively in Refs. 27 and 28, we will give only a brief description of the experiment.

The reactions are carried out in a 5 cm long, 3 mm i.d. open-ended glass sample cell, suspended in a 150 cm long by 7.5 cm i.d. gas cell. An approximately equimolar mixture of DI/H_2 at 4–5 Torr total pressure flows through the sample cell at a rate (0.20 Torr ℓs^{-1}) sufficient to replenish the reaction mixture between laser shots at the 10-pulse-per-second repetition rate of the pulsed lasers. A stream of argon enters the gas cell near the laser beam entrance and exit windows at the ends of the gas cell, to prevent the buildup of species on the windows. The total gas pressure is 11–12 Torr (7.0 Torr Ar plus the 4–5 Torr equimolar mixture of DI/H_2). The DI used in the experiments is synthesized by the reaction of D_2 with I_2 over a platinum catalyst.[36] A 2 ℓ atm sample was made a few hours ahead of the time the experiment was done. The purity of the DI sample was determined from DI and HI CARS spectra, and found to be greater than 95%.

A 5 ns FWHM UV laser pulse dissociates the DI in the mixture, producing translationally hot deuterium atoms. Two 5 ns FWHM visible laser pulses probe the H_2 and HD products 5 ns after the UV photolysis pulse, generating a CARS signal from the products. The DI photolysis wavelengths used in the present experiments are 266 and 280 nm, giving D + H_2 collision energies of 0.79 and 0.67 eV. The frequency-quadrupled output of a Nd:YAG laser provides the 266 nm light, while the frequency-doubled output of a tunable dye laser is the source of the 280 nm light. CARS[37] is a nonlinear process that requires two laser frequencies, the pump, ω_p, and a second, the Stokes, ω_s. In our experiments ω_p is fixed (Nd:YAG second harmonic), while ω_s (tunable Nd:YAG-pumped dye laser) is scanned to give the CARS spectrum. The CARS signal appears at the anti-Stokes frequency, $\omega_{as} = 2\omega_p - \omega_s$, where $\omega_r = \omega_p - \omega_s$, is the Raman transition frequency. Edge filters and a double monochromator spectrally and spatially separate ω_{as} from ω_s and ω_p. The CARS signal is detected by a photomultiplier tube, processed by a boxcar integrator, digitized, and recorded by a microcomputer.

The mean time between hard-sphere, elastic D + H_2 collisions is about 6 ns under the conditions of these experiments. This is calculated using a hard-sphere collision cross section of 9 Å^2 for D + H_2. Previous work done under similar conditions for H + D_2 at $E_{rel} = 1.30$ eV showed no discernible difference among HD product spectra taken with the CARS probe pulses delayed with respect to the photolysis pulse by less than 10 ns.[27] Thus, the present experiments, done with a 5 ns delay time, correspond effectively to single-collision conditions.

III. RESULTS

Figure 1 shows the vibrational Q-branch spectrum of the rotationally and/or vibrationally excited H_2 product formed by inelastic D + H_2 collisions at $E_{rel} = 0.79$ eV. The thermally populated reactant $v = 0, j = 4$ state peak, and the product peaks for $v' = 0, j' = 4, 5, 6, 7, 8$, and $v' = 1, j' = 1$ are plotted. The higher intensity for odd-j' peaks compared with that for even-j' peaks is a consequence of the different nuclear spin degeneracies, namely 3 for odd j' and 1 for even

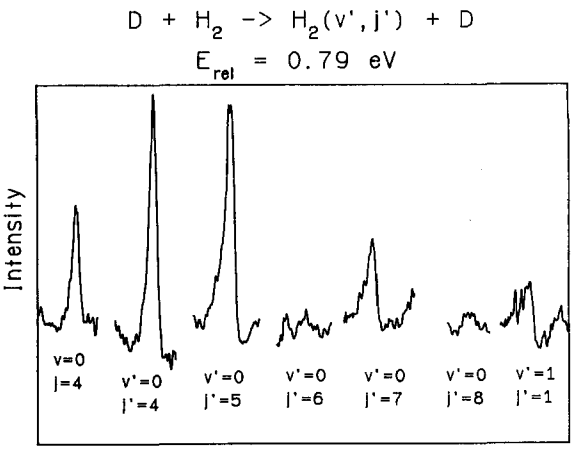

FIG. 1. The vibrational Q-branch CARS spectrum of the H_2 product from D + H_2 collisions at $E_{rel} = 0.79$ eV.

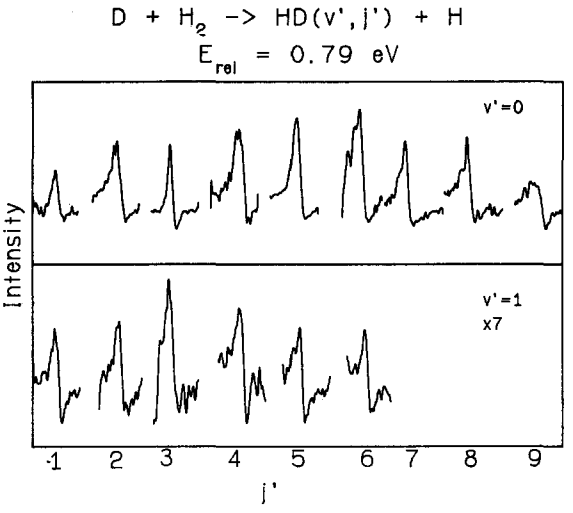

FIG. 2. The vibrational Q-branch CARS spectrum of the HD product from D + H_2 collisions at $E_{rel} = 0.79$ eV.

j'. The vibrational Q-branch spectrum of HD product formed by reactive D + H_2 collisions at the same energy is pictured in Fig. 2. The HD $v' = 0$, $j' = 1$–9 and $v' = 1$, $j' = 1$–6 product peaks are illustrated.

Since all the peaks in the spectra are well resolved, the CARS signal is given by[37]

$$S(\omega_{as}) = (c^4/\hbar\omega_s^4)^2(\Delta N)^2(d\sigma/d\Omega)^2 \times \int g(\omega;\omega_{as})F_2[(f')^2 + (f'')^2]d\omega + 2(c^4/\hbar\omega_s^4)(\Delta N)(d\sigma/d\Omega)\chi^{nr} \times \int g(\omega;\omega_{as})F_2 f' d\omega + (\chi^{nr})^2 \int g(\omega;\omega_{as})F_2\, d\omega \quad (2)$$

where ω_{as} and ω_s are the anti-Stokes and Stokes laser frequencies, $d\sigma/d\Omega$ is the Raman cross section for the transition, $g(\omega;\omega_{as})$ is the CARS laser line shape function centered at ω_{as}, F_2 is a factor dependent on the CARS laser frequencies and the focusing conditions, and f' and f'' are line shape functions of the real and imaginary parts of the third-order optical hyperpolarizability. Analysis of the spectra is done by generating $S(\omega_{as})$ from Eq. (2) for various ΔN, and comparing these with the experimental $S(\omega_{as})$ to determine the correct ΔN. From these $\Delta N(v',j') = N(v',j') - N(v'+1,j')$ we derive the $N(v',j')$ by setting $N(v',j')$ equal to zero for those states not energetically accessible.

Table I lists the relative populations derived from such an analysis for the H_2 and HD products of D + H_2 collisions at relative energies of 0.79 and 0.67 eV. The inelastic population distributions at both energies fall rapidly with increasing j'. For the inelastic H_2 product only 1 state in $v' = 1$ had a large enough population to be detected. Only an upper limit can be placed on the relative population of the H_2 product in $v' = 1, j' = 3$, namely 0.7 at 0.67 and 0.5 at 0.79 eV. It is difficult to establish even upper limits on the H_2 $v' = 1$, $j = 0$ and 2 populations, as a consequence of even-j' levels having a spin degeneracy three times smaller than the odd j'

TABLE I. Inelastic H_2 and reactive HD product quantum state distributions for D + H_2 collisions at 0.79 and 0.67 eV collision energy.

	Reactive HD $N(v',j')$	
v', j'	$E_{rel} = 0.67$ eV	$E_{rel} = 0.79$ eV
0, 1	8.6 ± 1.1	6.4 ± 1.0
0, 2	9.0 ± 1.2	8.4 ± 0.5
0, 3	9.1 ± 1.1	9.1 ± 1.1
0, 4	10.0 ± 1.0	9.9 ± 0.7
0, 5	7.8 ± 0.9	9.2 ± 0.3
0, 6	7.0 ± 1.0	10.0 ± 1.0
0, 7	4.6 ± 1.1	7.6 ± 0.6
0, 8	···	8.0 ± 1.0
0, 9	···	5.2 ± 0.8
1, 1	1.9 ± 0.4	0.8 ± 0.1
1, 2	2.1 ± 0.6	0.8 ± 0.1
1, 3	2.3 ± 0.5	1.2 ± 0.3
1, 4	2.0 ± 0.4	1.6 ± 0.1
1, 5	···	0.9 ± 0.1
1, 6	···	0.8 ± 0.1
	Inelastic H_2 $N(v',j')$	
v', j'	$E_{rel} = 0.67$ eV	$E_{rel} = 0.79$ eV
0, 4	10.0 ± 2.3	10.0 ± 2.2
0, 5	5.8 ± 0.9	5.5 ± 0.4
0, 6	3.9 ± 1.1	3.0 ± 0.9
0, 7	4.3 ± 0.6	2.8 ± 0.5
0, 8	···	2.1 ± 0.9
1, 1	1.6 ± 0.2	1.2 ± 0.2

levels. However, the absolute amount of $H_2(v' = 1)$ is not really small, because the absolute partial cross section for the state is larger than the partial cross section for any $v' = 1$ reactive product state. The CARS spectral region of the inelastic collision products has a large background contribution from nearby thermal reactant H_2 transitions. Thus, the sensitivity of the experiment for inelastic product is less than that for the reactive product, for which the CARS spectral region has a negligible background contribution from reactant H_2. At the higher collision energy H_2 states up to $v' = 0$, $j' = 10$ and $v' = 1, j' = 6$ are energetically allowed, while at the lower energy the limits are $v' = 0, j' = 9$, and $v' = 1$, $j' = 4$. At the 0.79 eV collision energy HD states up to $v' = 0, j' = 12$ and $v' = 1, j' = 8$ are energetically accessible, while at 0.67 eV states up to $v' = 0, j' = 11$ and $v' = 1$, $j' = 6$ are allowed. The reactive population distributions are plotted in Figs. 3 and 5, and the inelastic population distributions in Figs. 4 and 6, as points with $\pm$ one standard deviation error bars. The reactive population distributions at both energies show relatively broad rotational distributions that don't drop off as rapidly as their inelastic counterparts.

Our experiments also provide a measurement of the absolute cross sections[31] for these reactions, since absolute densities of both the reactants and the diatomic product can be made using CARS. The cross sections are given by

$$\sigma(v',j') = [H_2(v',j')]/([D][H_2]\Delta v_{rel}) \quad (3)$$

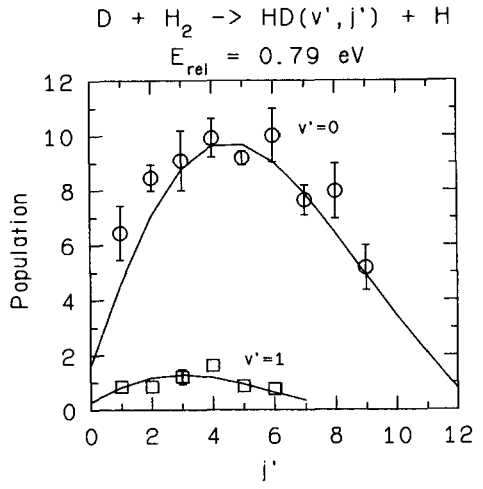

FIG. 3. Quantum state population distribution for HD formed in the $D + H_2 \rightarrow HD(v'j') + H$ reaction at a relative energy of 0.79 eV. The symbols are the experimental measurements, while the solid lines give the linear surprisal function with $\lambda_v = 2.2$, and $\theta_r = 2.5$ for $v' = 0$ and 2.0 for $v' = 1$. Error bars are equivalent to $\pm$ one standard deviation.

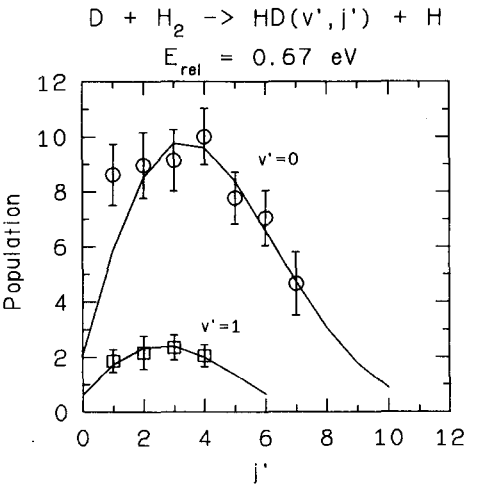

FIG. 5. Quantum state population distribution for HD formed in the $D + H_2 \rightarrow HD(v', j') + H$ reaction at a relative energy of 0.67 eV. The symbols are the experimental measurements and the solid lines give the linear surprisal function with $\lambda_v = 0.6$, and $\theta_r = 3.8$ for $v' = 0$ and 2.0 for $v' = 1$. Error bars are equivalent to $\pm$ one standard deviation.

and

$$\sigma(v', j') = [\mathrm{HD}(v', j')]/([D][\mathrm{H_2}]\Delta t v_{\mathrm{rel}}), \quad (4)$$

where [X] indicates a particle number density, Δt is the time between the UV photolysis pulse and the CARS probe pulses, and v_{rel} is the D + H_2 relative velocity. The collision velocity v_{rel} is given by

$$v_{\mathrm{rel}} = \sqrt{2E_{\mathrm{rel}}/\mu}, \quad (5)$$

where E_{rel} is the collision energy and μ is the reduced mass of D + H_2. The relative velocities are 1.25×10^6 cm s^{-1} for $E_{\mathrm{rel}} = 0.79$ eV and 1.14×10^6 cm s^{-1} for $E_{\mathrm{rel}} = 0.67$ eV. The time delay Δt is 5 ns. The number density of the H_2 reactant is known from a simple pressure measurement. Measurement of the CARS signals from the H_2 reactant calibrates the CARS spectral intensities and permits absolute measurement of the H_2 and HD product number densities.

The number density of deuterium atoms, [D], is given by

$$[\mathrm{D}] = [\mathrm{DI}]\, f_{\mathrm{photo}}\, f_{\mathrm{elec}}, \quad (6)$$

where [DI] is the DI number density, f_{photo} is the fraction of DI dissociated by the UV photolysis pulse (determined from the observed depletion of the DI CARS signal with the addition of the UV pulse), and f_{elec} is the quantum yield for the production of D + I($^2P_{3/2}$). The quantity f_{elec} is less than unity because dissociation of DI can lead to D + I($^2P_{3/2}$) or D + I($^2P_{1/2}$). For dissociation at 266 nm these two dissociation channels produce D atoms that give E_{rel} of 0.79 and 0.32 eV, respectively, while dissociation at 280 nm gives E_{rel} of

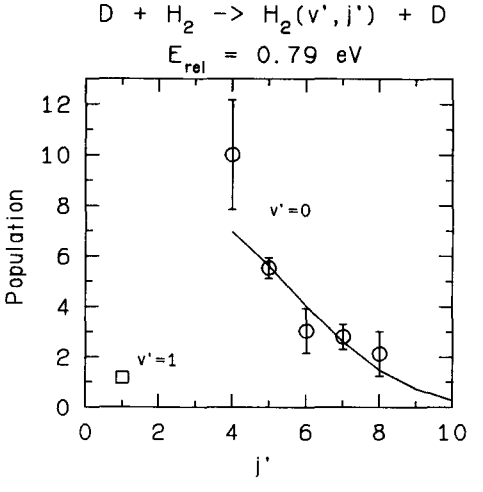

FIG. 4. Quantum state population distribution for H_2 product formed in inelastic D + H_2 collisions at a relative energy of 0.79 eV. The symbols are the experimental measurements and the solid line gives the linear surprisal function with $\theta_r = 4.4$. Error bars are equivalent to $\pm$ one standard deviation.

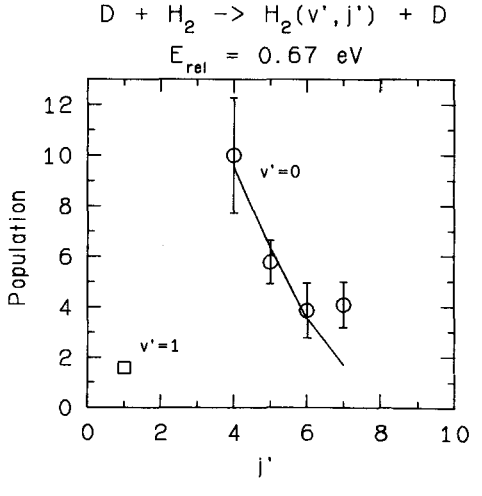

FIG. 6. Quantum state population distribution for H_2 product formed in inelastic D + H_2 collisions at a relative energy of 0.67 eV. The symbols are the experimental measurements, and the solid line gives the best fit linear surprisal with $\theta_r = 5.2$. Error bars are equivalent to $\pm$ one standard deviation.

TABLE II. Absolute partial cross sections for $D + H_2 \rightarrow H_2(v', j') + D$ at 0.67 and 0.79 eV collision energy.

	$\sigma(v', j')$, Å^2	
v', j'	$E_{rel} = 0.67$ eV	$E_{rel} = 0.79$ eV
0, 4	0.36 ± 0.13	0.37 ± 0.12
0, 5	0.21 ± 0.07	0.20 ± 0.06
0, 6	0.14 ± 0.05	0.11 ± 0.04
0, 7	0.16 ± 0.06	0.10 ± 0.03
0, 8	...	0.08 ± 0.03
1, 1	0.06 ± 0.02	0.04 ± 0.015

0.67 and 0.20 eV, respectively. For 266 nm photolysis of DI the quantum yield is 0.74 for $D + I(^2P_{3/2})$ and 0.26 for $D + I(^2P_{1/2})$.[38] Photolysis of DI at 280 nm leads to greater than 95% production of the $D + I(^2P_{3/2})$ channel.[38,39] The collision energies of the slower D atoms from the $D + I(^2P_{1/2})$ channel, 0.32 and 0.20 eV, are below the reaction threshold,[7-12] and therefore of no significance for the exhange reaction. These slower D atoms produced in 266 nm DI photolysis can, however, contribute to inelastic, particularly rotationally inelastic, collisions, and our measured H_2 product population distributions must contain some contribution from them. However, even if the excitation cross section in $D + H_2$ collisions at 0.32 eV were to be as large as at 0.79 eV, the slower D atoms could contribute no more than 17% of the inelastic H_2 product. For 0.32 eV collision energy H_2 states only up to $v' = 0, j' = 6$ are accessible.

The absolute partial cross sections we derive are listed in Tables II and III. The additional measurements needed to calculate the absolute partial cross sections lead to larger uncertainty in them in the relative populations. The major sources of the additional uncertainty are associated with measurement of the degree of DI photolysis, measurement of the pressure of the DI, and uncertainty in the time delay.

TABLE III. Absolute partial cross sections for $D + H_2 \rightarrow HD(v', j') + H$ at 0.67 and 0.79 eV collision energy.

	$\sigma(v', j')$, Å^2	
v', j'	$E_{rel} = 0.67$ eV	$E_{rel} = 0.79$ eV
0, 1	0.097 ± 0.033	0.064 ± 0.022
0, 2	0.100 ± 0.034	0.084 ± 0.028
0, 3	0.102 ± 0.035	0.089 ± 0.030
0, 4	0.112 ± 0.038	0.097 ± 0.033
0, 5	0.087 ± 0.029	0.090 ± 0.030
0, 6	0.078 ± 0.027	0.097 ± 0.033
0, 7	0.051 ± 0.021	0.074 ± 0.025
0, 8	...	0.077 ± 0.026
0, 9	...	0.050 ± 0.017
1, 1	0.021 ± 0.007	0.009 ± 0.003
1, 2	0.024 ± 0.008	0.009 ± 0.003
1, 3	0.026 ± 0.009	0.012 ± 0.004
1, 4	0.023 ± 0.008	0.016 ± 0.005
1, 5	...	0.008 ± 0.003
1, 6	...	0.007 ± 0.002

Of particular note with regard to these partial cross sections is the fact that both the HD and H_2 $v' = 1$ product cross sections are larger at the lower of the two collision energies. For the inelastic product the difference between the $\sigma(v' = 1)$ at the 0.67 and 0.79 eV collision energies is within experimental uncertainty, but the $\sigma(v' = 1)$ difference is quite large and definitely significant for the reactive product. The enhancement of $v' = 1$ HD production relative to $v' = 0$ HD is also clearly evident in the population distributions of Table I and Figs. 3 and 5. We believe this is evidence for a Feshbach resonance in $D + H_2$ collisions, a contention discussed more fully in the next section.

We have calculated the fractional energy disposal for the product energy distributions in the reactive HD product of $D + H_2$ collisions at the two energies studied. The results are listed in Table IV, together with the energy disposal that characterizes the results of some of our previous experiments with other isotopic variants of the hydrogen exchange reaction. In all cases 69%–84% of the energy appears in translation, 8%–25% is in rotation, and 2%–10% is in vibration. The energy disposal for $D + H_2 \rightarrow HD + H$ shows the considerable enhancement of product vibration at the lower of the two collision energies studied, where we believe a Feshbach resonance is operative. Feshbach resonances in $H + p$-H_2 at 0.70 and 1.00 eV collision energy also are accompanied by an increase in f'_{vib} relative to off-resonance collision energies 0.79 and 1.10 eV.

While the fractional energy disposal provides a convenient and simple description of the product rotational and vibrational distributions, a linear surprisal analysis[40-42] provides a more useful parametrization of these distributions. The surprisal analysis involves comparing the observed product state distributions with a common reference distribution, a statistical distribution in which all product states are equally probable. The provision of a common reference "frame" allows direct and meaningful comparison of the $H + H_2$ reaction dynamics at different energies and for different isotopic variants of the reaction, helping to identify

TABLE IV. Energy disposal in three isotopic variants of the hydrogen exchange reaction

	E_{rel}	f'_{trans} [a]	f'_{rot} [b]	f'_{vib} [c]
$D + H_2 \rightarrow HD + H$ [d]	0.67 eV	0.71	0.19	0.10
	0.79 eV	0.70	0.25	0.05
$H + D_2 \rightarrow HD + D$ [e]	0.98 eV	0.73	0.21	0.06
	1.10 eV	0.74	0.22	0.04
	1.30 eV	0.69	0.24	0.07
$H + p$-$H_2 \rightarrow H_2 + H$ [f]	0.70 eV	0.83	0.08	0.09
	0.79 eV	0.84	0.12	0.04
	1.00 eV	0.78	0.16	0.06
	1.10 eV	0.82	0.16	0.02

[a] The fraction of the total available energy in product translation.
[b] The fraction of the total available energy in product rotation.
[c] The fraction of the total available energy in product vibration.
[d] This work.
[e] References 27 and 28.
[f] References 24 and 25.

how isotopic and energetic variations alter the dynamical bias of the reaction. This is the principal advantage of the surprisal analysis, and the primary reason for our use of it. The utility of this information theory approach has been demonstrated in the analysis of our previous results for the H + D$_2$ and H + H$_2$ variants of the hydrogen exchange reaction.[25–30,42]

The statistical, or prior, distribution that provides the common reference in the surprisal analysis is, for an atom plus diatom reaction, given by

$$P^0(v',j') = \frac{(2j'+1)(E-E_r-E_v)^{1/2}}{\Sigma_{v'}\Sigma_{j'}(2j'+1)(E-E_r-E_v)^{1/2}}, \quad (7)$$

where E is the total energy, and E_v and E_r are the vibrational and rotational energies of the diatom. $P^0(v',j')$ is simply the number of states with quantum numbers v' and j', divided by the total number of product states energetically accessible. The product distributions are related to this prior distribution via the linear surprisal parameters, λ_v and θ_r, for the vibration and rotation, respectively, of the product diatom,

$$P(v',j') = P^0(v',j')\exp(-\lambda_0 - \lambda_v f_v - \theta_r g_r). \quad (8)$$

The parameters f_v and g_r are the fractions of the energy in vibration and rotation, $f_v = E_v/E$ and $g_r = E_r/(E-E_v)$, and λ_0 is a scale factor.

The prior distribution used in this formulation lacks the constraint of conservation of total angular momentum. While in principle this is a serious deficiency, in practice it does not remove the utility of the linear surprisal description. However, as a consequence of this omission, the value of the rotational surprisal parameter θ_r may reflect the angular momentum conservation constraint that is lacking in the statistical (reference) distribution. For our purposes any such influence on θ_r does nothing to diminish its usefulness, since we invoke it simply as a convenient parametrization of the product rotational state distribution, a parametrization that allows systematic intercomparison of the rotational state distributions in the various experiments we have carried out on the hydrogen exchange reaction. That is, we interpret the surprisal parameters largely in terms of their values relative to one another.

Linear least-squares fitting of the surprisal function of Eq. (8) to our $H_2^\dagger$ and HD product quantum state distributions yields the solid lines shown in Figs. 3–6. In all cases the simple linear surprisal function provides a good description of the measurements. For the inelastic product of D + H$_2$ collisions at $E_{rel} = 0.67$ and 0.79 eV we find $\theta_r = 5.2 \pm 1.10$ and 4.4 ± 0.2 for $v' = 0$. While the linear rotational surprisal function describes the measured inelastic H$_2$ product distributions reasonably well, the use of the surprisal function to extrapolate the product populations to higher and lower j' than observed is not recommended. There are simply too few measured $H_2(v'=0,j')$ populations to yield a θ_r that we can be confident enough of to allow such extrapolation. For D + H$_2$ reactive collisions at $E_{rel} = 0.79$ eV we find linear rotational surprisal parameters $\theta_r = 2.5 \pm 0.1$ for $v' = 0$ and $\theta_r = 2.0 \pm 0.3$ for $v' = 1$. At $E_{rel} = 0.67$ eV we find $\theta_r = 3.8 \pm 0.50$ for $v' = 0$ and 2.0 ± 0.4 for $v' = 1$. The inelastic D + H$_2$ collisions at both energies show more bias against rotation than the reactive D + H$_2$ collisions. We have also found this behavior for the H + p − H$_2$ and H + D$_2$ collisions that we have studied previously.[25–30]

The vibrational surprisal parameters that best describe the inelastic data are $\lambda_v = 0.74 \pm 0.2$ at 0.67 eV and $\lambda_v = 1.3 \pm 0.2$ at 0.79 eV. However, since we have been able to observe product in only a single rotational state of $v' = 1$, the vibrational state distribution of the H$_2$ product is not well determined. For reactive D + H$_2$ collisions the larger number of $v' = 1$ product rotational states observed makes it easier to determine λ_v. For 0.67 eV we find $\lambda_v = 0.6 \pm 0.2$ while at 0.79 eV this is 2.2 ± 0.2. Note the significant decrease in λ_v at the lower collision energy, reflecting a relaxation of the dynamical bias against product vibrational excitation. Since the linear suprisal function provides a good description of our HD product quantum state distributions, we can use the surprisal function to determine $N(v',j')$ and $\sigma(v',j')$ for those v',j' states not actually observed in the experiment. This allows us to compute a total reaction cross section, summed over v' and j', even though there are missing states in our measurements. We find that the total cross section at both 0.67 and 0.79 eV relative energies is 0.81 ± 0.35 Å^2. The $N(v',j')$ represented by the linear surprisal functions are also used to calculate the fractional energy disposal data given in Table IV.

IV. DISCUSSION

A. Dynamical resonance behavior

As the collision energy is lowered from $E_{rel} = 0.79$ eV to $E_{rel} = 0.67$ eV the energy available to the products of the D + H$_2$→HD + H reaction goes down, and it would be reasonable to expect the product distributions to shift to lower v',j' states at the lower collision energy. The H$_3$ potential energy surface[43,44] has a minimum barrier for collinear geometry, and the barrier height increases rapidly with decreasing H–H–H angle, from about 0.40 eV for 180° to about 1.3 eV for 90°.[44] Therefore, as the collision energy is deceased the reactive collisions become more constrained to near-collinear geometries and smaller impact parameters, both of which should favor less product rotational excitation. The predominant vibrational adiabaticity[45] for the hydrogen exchange reaction also suggests decreasing vibrational excitation with decreasing collision energy.

The product distributions in Figs. 3 and 5 show the expected trend for rotational excitation, but the vibrational excitation at the lower collision energy is greater than that in the higher collision energy experiment. This is apparent in the $\sigma(v',j')$ partial cross sections as well. This type of behavior could indicate oscillatory, or resonance like, $\sigma(v')$ partial cross sections. The *increase* in the relative, as well as the absolute, yield of the HD($v' = 1$) product of the D + H$_2$ reaction that accompanies a small *decrease* in the relative energy is the most significant observation of this study, for we believe this to be the result of a dynamical resonance in the reaction at about 0.65 eV. There is evidence to suggest that this interpretation is correct.

A Feshbach resonance in any isotopic variant of the hydrogen exchange reaction is expected just above the energetic threshold for the $v' = 1$ product.[8–11,46] Recent calculations by Webster and Light[10] indicate that the threshold for the

$D + H_2(v=0) \rightarrow HD(v'=1) + H$ reaction is at 0.61 eV relative energy. These calculations also show a peak in the $v'=1$ cross section and a dip in the $v'=0$ cross section at $\approx$0.67 eV relative energy, which is likely to be the result of the expected Feshbach resonance. The $n=1$ vibrationally adiabatic potential energy surface[47] for DH_2 shows a well that could support the quasibound state necessary to produce the Feshbach resonance internal excitation state. In our previous experiments on $H + H_2$ we found a strong Feshbach resonance at 0.70 eV collision energy, about 0.04 eV above the $v'=1$ product threshold, almost exactly where it was predicted theoretically.[9–11,13,48–51] The behavior expected for a Feshbach resonance just above the $v'=1$ product threshold—an enhancement in the $v'=1$ cross section—is precisely what we observe for both $D + H_2$ and $H + H_2$. Of course, quantum coupled channel calculations also predict a decrease in the $v'=0$ product cross section at the resonance, and this we do not observe, either for $D + H_2$ or $H + H_2$. However, these calculations have been carried out only for $J=0$ total angular momentum,[7–11] and, for $H + H_2$, for selected $J \leqslant 2$.[13,48–51]

We believe that it is possible to observe the Feshbach resonances that occur just above a particular product vibrational state threshold in the hydrogen exchange reaction because there are only a few partial waves contributing to the near-threshold product vibrational state. As a consequence, the partial wave sum is not so extensive as to wash out the resonance in the partial cross section for that vibrational state. However, for the reaction to produce lower vibrational states, which are already far above threshold, there are undoubtedly many partial waves contributing and the partial wave sum does apparently wash out the resonance effects. Some evidence to support this view comes from an examination of the rotational distributions of the $HD(v'=1)$ product of the $D + H_2(v=0)$ reaction at 0.79 and 0.67 eV, shown in Table III. The resonance enhancement appears to occur primarily in the lower rotational states of $v'=1$. To the extent that there is angular momentum coupling between the reactant orbital angular momentum and the product rotational angular momentum, this observation would suggest that it is only partial waves of low orbital angular momentum that are contributing significantly to the resonance.

TABLE V. Rotational surprisal parameters for collisions of hydrogen atoms with hydrogen molecules.

Collision type	E_{rel}		θ_r Reactive	θ_r Inelastic
$D + H_2$	0.67 eV	$v'=0$	3.8	5.2
		$v'=1$	2.0	···
	0.79 eV	$v'=0$	2.5	4.3
		$v'=1$	2.0	···
$H + D_2$	0.98 eV	$v'=0$	3.5	···
		$v'=1$	3.5	···
	1.10 eV	$v'=0$	3.4	···
		$v'=1$	3.0	6.4
	1.30 eV	$v'=0$	3.0	···
		$v'=1$	3.0	5.9
		$v'=2$	···	6.9
$H + H_2$	0.70 eV	$v'=0$	10.8	9.3
	0.79 eV	$v'=0$	7.6	9.4
	1.00 eV	$v'=0$	5.1	9.0
	1.10 eV	$v'=0$	5.5	7.5

The increase in the $D + H_2$ $v'=1$ reactive cross section between 0.79 and 0.67 eV is accompanied by a similar, but smaller increase in the $v'=1$ inelastic cross section. As the data in Tables I and II show, the 33% increase in the relative cross section for $H_2(v'=1)$, is just barely significant, but, due to the larger uncertainties, this same percent increase is not statistically significant in the absolute partial cross section. Our evidence of the effect of the resonance on the inelastic cross section is thus much weaker than that for the effect on the reactive cross section. However, the effect we do see is consistent with the expectation that this particular Feshbach resonance should enhance the production of both $HD(v'=1)$ and $H_2(v'=1)$ in $D + H_2(v=0)$ collisions. The enhancement of $H_2(v'=1)$ should probably be less than that for $HD(v'=1)$, because the barrier to decay of the DH_2 quasi-bound state is greater for $D + H_2(v'=1)$ products than for $H + HD(v'=1)$ products as a result of the greater vibrational energy of $H_2(v'=1)$.

The Feshbach resonances result from excitation of the transition state to excited states of the vibrational degrees of freedom perpendicular to the reaction coordinate. The particular resonance that should occur just above the $v'=1$ product threshold has been assigned to the first excited state of the symmetric stretch motion in the $[H_3]^\dagger$ transition state.[48–51] In the $[DH_2]^\dagger$ transition state this resonant state may involve a similar vibrational motion, although it could no longer be called a symmetric stretch, because of the reduced symmetry. In any case, this vibrationally excited transition state can decay to products or to reactants, so its production should enhance both the vibrationally nonadiabatic reactive scattering and the inelastic scattering. There are no quantum calculations on the inelastic collisions of $D + H_2$ that we are aware of, at least no calculations at relative energies around 0.6–0.8 eV, where the Feshbach resonance appears to be. Consequently, there are no theoretical predictions about the relative effect of the resonance on the $v'=1$ inelastic and reactive cross sections. However, for $H + H_2$ recent coupled channel calculations for $J=0$ total angular momentum by Hipes and Kuppermann[11] show an enhancement of both the reactive $v'=1$ transition probability and the inelastic $v'=1$ transition probability. In fact this is what we observe in our $H + H_2$ experiments.[24,25]

B. Angular momentum coupling

Table V summarizes the rotational surprisal parameters in the product distributions for some of the experiments we have carried out for three isotopic combinations, $H + p\text{-}H_2$, $H + D_2$, and $D + H_2$, in these hydrogen atom–hydrogen molecule collisions. In all of the systems and at all the energies we have studied there is a relatively strong and consistent bias against rotational excitation, as indicated by the positive rotational surprisal parameters in Table V. However, there is also a difference in the degree of this bias. The

bias against rotational excitation follows the order $H + p\text{-}H_2 > H + D_2 > D + H_2$. The extent of the bias against rotational excitation for a particular isotopic combination is fairly constant over the somewhat limited energy range of our experiments. For example, for $H + D_2 \rightarrow HD + D$ at relative energies between 0.98 and 1.30 eV, the rotational surprisal parameters are in the range of 3.0–3.5. For $H + p\text{-}H_2 \rightarrow o\text{-}H_2 + H$ reaction over the same energy regime the rotational surprisal parameters range from 5.0 to 5.5, while at lower collision energies, around 0.75 eV, the rotational surprisal parameters are 8 to 11. At these lower collision energies the $D + H_2$ system shows less bias against rotational excitation than the other two isotopic combinations. $D + H_2 \rightarrow HD + H$ has rotational surprisal parameters from 2.0 to 3.8 with three of four between 2.0 and 2.5.

The rotational surprisal parameters should not be over interpreted. Some of the difference among the θ_r values for the $H + p\text{-}H_2$, $H + D_2$, and $D + H_2$ systems is certainly a consequence of the different total angular momenta in these systems. Since the surprisal analysis uses a prior distribution that is not constrained by conservation of total angular momentum, two systems with identical dynamics will give different θ_v if they have different total angular momenta. We can estimate the total angular momenta in these collisions, based on our measurements of the total reaction cross sections, and gauge the importance of the total angular momentum constraint.

For the H_2 and D_2 reactants at room temperature $\langle j' \rangle$ is only 1 or 2, so the total angular momentum J is dominated by the reactant orbital angular momentum l, i.e., $J \approx l$. The orbital angular momentum can be related to the total cross section by the classical relations $l = \mu v_{rel} b$ and $\sigma = \pi b^2$, giving

$$J \approx l = \mu(2E_{rel}/\mu)^{1/2}(\sigma/\pi)^{1/2} = (2/\pi)^{1/2}(\mu E_{rel}\sigma)^{1/2}.$$

At a given energy the reaction cross sections are in the order $\sigma(D + H_2) > \sigma(H + H_2) > \sigma(H + D_2)$ as a consequence of zero-point energy differences, while $\mu(D + H_2) > \mu(H + D_2) > \mu(H + H_2)$. Thus, the total angular momentum available in the $D + H_2$ reaction is greater than in the other two isotopic variants, and we expect this reaction to give "hotter" rotational distributions than the other two. However, the rotational distributions we measure do not have $\langle j' \rangle$ that scale simply as $(\mu E_{rel}\sigma)^{1/2}$, and the rotational surprisal parameters do reflect changing dynamics in the hydrogen exchange reaction with changes in isotopes.

The same trend in the bias against rotational excitation is found in the inelastic collisions as in the reactive collisions. For a given isotopic variant the bias against product rotational excitation is generally stronger for inelastic than for the reactive collisions. Comparing the θ_r for the inelastic collisions of the different isotopic variants we find again $H + p\text{-}H_2 > H + D_2 > D + H_2$.

C. Comparison with classical trajectory calculations

In Figs. 7 and 8 we compare the product quantum state distributions for $D + H_2 \rightarrow HD + H$ that we have measured with state distributions from the QCT calculations of Blais and Truhlar.[52] The QCT calculations were carried out at several relative energies, but not at the 0.67 or 0.79 eV energies of our experiments. In order to make comparison with the experimental results we have linearly interpolated and extrapolated the 0.70 and 0.85 eV data of Blais and Truhlar. These are the two energies at which the calculations have been done that are closest to the energies of the experiments. In order to make the comparison of relative population distributions shown in Figs. 7 and 8 meaningful, we scale the QCT data such that $\Sigma_{v'} \Sigma_{j'} N(v', j')$ is the same for it and the experimental data.

Comparing relative population distributions the QCT results are in almost as good agreeent with experiment for $D + H_2 \rightarrow HD + H$ at these relatively low collision energies as they are[26–33] for $H + D_2 \rightarrow HD + D$ at higher collision energies. Note that at 0.79 eV the calculations give f'_{vib}

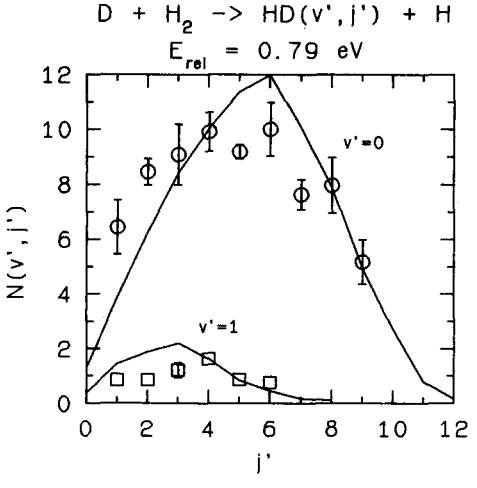

FIG. 7. Comparison of the experimental $HD(v', j')$ product quantum state distribution (symbols $\pm$ one standard deviation) for the $D + H_2 \rightarrow HD(v', j') + H$ reaction at $E_{rel} = 0.79$ eV with the distribution (solid line) derived from the quasiclassical trajectory calculations of Blais and Truhlar (Ref. 52).

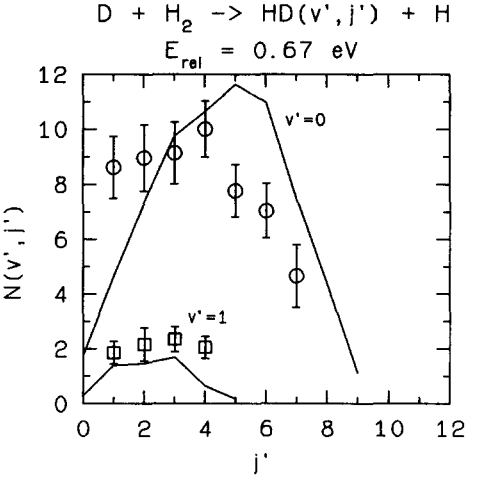

FIG. 8. Comparison of the experimental $HD(v', j')$ product quantum state distribution (symbols $\pm$ one standard deviation) for the $D + H_2 \rightarrow HD(v', j') + H$ reaction at $E_{rel} = 0.67$ eV with the state distribution (solid line) derived from the quasiclassical trajectory calculations of Blais and Truhlar (Ref. 52).

$= 0.056$, $f'_{rot} = 0.242$, and $f'_{trans} = 0.702$, in very good agreement with the experimental results given in Table IV. At 0.67 eV relative energy there are noticeable differences between the QCT results and the measurements. The calculations give a $v' = 0$ rotational distribution that seems peaked at about $1\hbar$ higher than the experimental one. More importantly, the calculations give too little $v' = 1$ relative to $v' = 0$. This shows up in the average energy disposal, the trajectories giving $f'_{vib} = 0.048$, $f'_{rot} = 0.211$, and $f'_{trans} = 0.741$. This f'_{vib} is only half the measured value, given in Table IV.

Comparing absolute partial cross sections (Tables VI and VII) we find that the agreement between the QCT results and the measurements is not as good. Even though the uncertainty in the absolute cross section measurements is considerable, typically $\pm$ 33% for one standard deviation, the QCT cross sections are systematically larger than the measured values by an amount exceeding the experimental uncertainty. The only exception occurs for $v' = 1$ at 0.67 eV, for which the QCT and experimental cross sections are very close. This discrepancy is of course also reflected in the total cross sections. For the QCT data the total sections are 0.99 and 1.23 Å^2 at 0.67 and 0.79 eV, while the measured values are both 0.81 ± 0.35 Å^2.

Previously we found[31] good agreement between QCT calculated and experimental partial cross sections for $H + D_2 \rightarrow HD + D$ at relative energies between 0.98 and 1.30 eV. Even the more accurate ($\pm$ 10%) total cross section measurements of Johnston *et al.*[53] for $H + D_2 \rightarrow HD + D$ between 0.9 and 2.5 eV were in good agreement with the QCT total cross sections.[32,33,54–56] The discrepancy between the QCT and experimental partial cross sections for $D + H_2 \rightarrow HD + H$ at these relatively low collision energies may simply reflect the breakdown of classical mechanics at energies approaching threshold. Note that partial cross sections from QCT calculations[32] for $H + D_2 \rightarrow HD + D$ at 0.55 eV relative energy are about 60% larger than those from accurate quantum calculations.[57]

The QCT results lend credence to our belief that a Feshbach resonance is present at $\approx$0.65 eV. The QCT calculations, which should not show resonance effects, have f'_{vib} and $\sigma(v' = 1)$ decreasing from 0.79 to 0.67 eV, the "normal" behavior. The experimental f'_{vib} and $\sigma(v' = 1)$ increase from 0.79 to 0.67 eV, exactly opposite and precisely the expected resonance behavior.

D. Comparison with crossed molecular beam experiments

Buntin, Giese, and Gentry[34,35] have reported a crossed molecular beam study of the $D + H_2 \rightarrow HD + H$ reaction in which they measured the product velocity distribution for directly backscattered product, and used this to deduce the rotational–vibrational population distributions of the backscattered HD product. The beam experiments have been done only at collision energies higher than our experiments, 0.85 to 1.20 eV, and the beam results are for product scattered into a narrow range of center-of-mass angles around 180°, while we measure the angle-averaged cross sections. Thus, the two experiments cannot be compared at the level of detail each provides. However, the results of the CARS and beam experiments are at least qualitatively the same. The 0.85 eV molecular beam data gives a broader rotational distribution than the 0.79 eV CARS data, but the mean j' values are similar. In $v' = 0$ we find $\langle j' \rangle = 4.8 \pm 0.3$, while the beam results give 5.7 ± 0.4. In $v' = 1$ we measure $\langle j' \rangle = 3.6 \pm 0.6$, while the beam results give 2.5 ± 1.7. Our spectroscopic measurements indicate that $N(v' = 1)/$

TABLE VI. Absolute partial cross sections for $D + H_2 \rightarrow HD(v', j') + H$ at 0.79 eV collision energy.

	$\sigma(v', j')$, Å^2	
v', j'	Experiment	QCT[a]
0, 0	···	0.0178
0, 1	0.064 ± 0.022	0.0523
0, 2	0.084 ± 0.028	0.0869
0, 3	0.089 ± 0.030	0.1160
0, 4	0.097 ± 0.033	0.1390
0, 5	0.090 ± 0.030	0.1570
0, 6	0.097 ± 0.033	0.1660
0, 7	0.074 ± 0.025	0.1390
0, 8	0.077 ± 0.026	0.1090
0, 9	0.050 ± 0.017	0.0684
0, 10	···	0.0374
0, 11	···	0.0109
0, 12	···	0.0023
1, 0	···	0.0053
1, 1	0.009 ± 0.003	0.0199
1, 2	0.009 ± 0.003	0.0261
1, 3	0.012 ± 0.004	0.0306
1, 4	0.016 ± 0.005	0.0224
1, 5	0.008 ± 0.003	0.0116
1, 6	0.007 ± 0.002	0.0063
1, 7	···	0.0024
1, 8	···	0.0013

[a] Reference 52, linear interpolation from data for $E_{rel} = 0.70$ and 0.85 eV.

TABLE VII. Absolute partial cross sections for $D + H_2 \rightarrow HD(v', j') + H$ at 0.67 eV collision energy.

	$\sigma(v', j')$, Å^2	
v', j'	Experiment	QCT[a]
0, 0	···	0.0229
0, 1	0.097 ± 0.033	0.0607
0, 2	0.100 ± 0.034	0.0964
0, 3	0.102 ± 0.035	0.1280
0, 4	0.112 ± 0.038	0.1400
0, 5	0.087 ± 0.029	0.1530
0, 6	0.078 ± 0.027	0.1440
0, 7	0.051 ± 0.021	0.0984
0, 8	···	0.0576
0, 9	···	0.0146
1, 0	···	0.0038
1, 1	0.021 ± 0.007	0.0183
1, 2	0.024 ± 0.008	0.0193
1, 3	0.026 ± 0.009	0.0222
1, 4	0.023 ± 0.008	0.0085
1, 5	···	0.0022

[a] Reference 52, linear extrapolation from data for $E_{rel} = 0.70$ and 0.85 eV.

$N(v'=0)$ is $0.092+0.012/-0.008$m while the molecular beam data have this ratio equal to $0.083+0.028/-0.016$.

V. CONCLUSION

We have measured relative population distributions and absolute partial cross sections for the reactive and inelastic products of $D+H_2$ collisions at relative collision energies of 0.67 and 0.79 eV. The observed energy disposal is similar to that in the analogous $H+H_2$ and $H+D_2$ reactions and energy transfer.

The observed *increase* in both the relative and absolute production of $HD(v'=1)$ from $D+H_2$ collisions that occurs upon a very small *decrease* in the relative collision energy from 0.79 to 0.67 eV is evidence of dynamical resonance behavior in the $D+H_2$ reaction. Also observed is a similar but smaller increase in the production of the inelastic $H_2(v'=1)$ product at the lower energy. A dynamical, or Feshbach, resonance in this reaction just above the $v'=1$ threshold would be expected to enhance the production of $HD(v'=1)$ and $H_2(v'=1)$ from $D+H_2(v'=0)$ collisions, consistent with our observations.

Quasiclassical trajectory calculations provide product quantum state distributions that are in reasonable agreement with those measured here. However, the QCT derived absolute partial cross sections are generally larger than those measured. Some discrepancy between the QCT calculations and the experimental measurements is evident even in the relative population distributions at 0.67 eV collision energy. If a dynamical resonance is influencing the dynamics at this energy such discrepancy is not unexpected.

ACKNOWLEDGMENT

This work is supported by Grant Nos. CHE-8506010 and CHE-8810557 from the National Science Foundation.

[1]D. G. Truhlar and R. E. Wyatt, Annu. Rev. Phys. Chem. **27**, 1 (1976).
[2]*Atom–Molecular Collision Theory*, edited by R. B. Bernstein (Plenum, New York, 1979).
[3]R. B. Walker and J. C. Light, Annu. Rev. Phys. Chem. **31**, 401 (1980).
[4]A. Kuppermann, Theor. Chem. Adv. Prespect **A6**, 79 (1981).
[5]M. Baer, Adv. Chem. Phys. **49**, 191 (1982).
[6]G. C. Schatz, in *The Theory of Chemical Reaction Dynamics*, edited by D. C. Clary (Reidel, Dordrecht, 1986), pp. 1–26 and references therein.
[7]A. B. Elkowitz and R. E. Wyatt, J. Chem. Phys. **62**, 2504 (1975); **63**, 702 (1975).
[8]G. C. Schatz and A. Kuppermann, J. Chem. Phys. **65**, 4642, 4668 (1976).
[9]R. B. Walker, E. B. Stechel, and J. C. Light, J. Chem. Phys. **69**, 2922 (1978).
[10]F. Webster and J. C. Light, J. Chem. Phys. **85**, 4744 (1986).
[11]P. G. Hipes and A. Kuppermann, Chem. Phys. Lett. **133**, 1 (1987).
[12]R. T Pack and G. A. Parker, J. Chem. Phys. **87**, 3888 (1987).
[13]M. Mladenovic, M. Zhao, D. G. Truhlar, D. W. Schwenke, Y. Sun, and D. J. Kouri, Chem. Phys. Lett. **146**, 358 (1988).
[14]K. Haug, D. W. Schwenke, Y. Shima, D. G. Truhlar, J. Zhang, and D. J. Kouri, J. Phys. Chem. **90**, 6757 (1986).
[15]T. Takayanagi, N. Masaki, N. Makoto, S. Sato, and G. C. Schatz, J. Chem. Phys., **86**, 6133 (1987).
[16]T. Miyazaki and K. Lee, J. Phys. Chem. **90**, 400 (1986).
[17]T. Miyazaki, K. Lee, F. Fueki, and A. Takeuchi, J. Phys. Chem. **88**, 4959 (1984).
[18]H. Tsuruta, T. Miyazaki, F. Fueki, and N. Azuma, J. Phys. Chem. **87**, 5422 (1983).
[19]A. V. Ivliev, A. S. Iskovskikh, A. Y. Katunin, I. I. Lukashevich, V. V. Suraev, V. V. Filippov, N. I. Filippov, and V. A. Shevatsov, JETP Lett. **38**, 379 (1983).
[20]D. G. Truhlar, A. Kuppermann, and J. T. Adams, J. Chem. Phys. **59**, 395 (1973).
[21]B. C. Garrett and D. G. Truhlar, J. Chem. Phys. **72**, 3460 (1980).
[22]A. Kuppermann, in *Potential Energy Surfaces and Dynamics Calculations*, edited by D. G. Truhlar (Plenum, New York, 1981), p. 375.
[23]*Resonances*, edited by D. G. Truhlar ACS Symp. Ser. 263 (American Chemical Society, Washington, D.C., 1984).
[24]J.-C. Nieh and J. J. Valentini, Phys. Rev. Lett. **60**, 519 (1988).
[25]J.-C. Nieh and J. J. Valentini, J. Chem. Phys. (submitted)
[26]D. P. Gerrity and J. J. Valentini, J. Chem. Phys. **79**, 5202 (1983).
[27]D. P. Gerrity and J. J. Valentini, J. Chem. Phys. **81**, 1298 (1984).
[28]D. P. Gerrity and J. J. Valentini, J. Chem. Phys. **82**, 1323 (1985).
[29]D. P. Gerrity and J. J. Valentini, J. Chem. Phys. **83**, 2207 (1985).
[30]J. J. Valentini and D. P. Gerrity, Int. J. Chem. Kinet. **18**, 937 (1986).
[31]H. B. Levene, D. L. Phillips, J.-C. Nieh, D. P. Gerrity, and J. J. Valentini, Chem. Phys. Lett. **143**, 317 (1988).
[32]N. C. Blais and D. G. Truhlar, Chem. Phys. Lett. **102**, 120 (1983).
[33]N. C. Blais and D. G. Truhlar, J. Chem. Phys. **83**, 2201 (1985).
[34]S. A. Buntin, C. F. Giese, and W. R. Gentry, J. Chem. Phys. **87**, 1443 (1987).
[35]S. A. Buntin, Ph.D. thesis, University of Minnesota, 1988.
[36]D. Rittenberg and H. C. Urey, J. Am. Chem. Soc. **56**, 1885 (1934).
[37]For a review of CARS see J. J. Valentini, in *Spectrometric Techniques*, edited by G. A. Vanasse (Academic, New York, 1985), Vol. 4, Chap. 1.
[38]R. D. Clear, S. J. Riley, and K. R. Wilson, J. Chem. Phys. **63**, 1340 (1975).
[39]G. N. A. Van Veen, K. A. Mohamed, T. Baller, A. E. DeVries, Chem. Phys. **80**, 113 (1983).
[40]R. B. Bernstein and R. D. Levine, Adv. At. Mol. Phys. **11**, 215 (1975).
[41]R. D. Levine and R. B. Bernstein, Acc. Chem. Res. **7**, 393 (1974).
[42]E. Zamir, R. D. Levine, and R. B. Bernstein, Chem. Phys. Lett. **107**, 217 (1984).
[43]P. Siegbahn and B. Liu, J. Chem. Phys. **68**, 2457 (1978).
[44]D. G. Truhlar and C. J. Horowitz, J. Chem. Phys. **68**, 2466 (1978); **71**, 1514 (E) 1979.
[45]R. A. Marcus, J. Chem. Phys. **43**, 1598 (1965).
[46]J. Manz, E. Pollak, and J. Romelt, Chem. Phys. Lett. **86**, 26 (1982).
[47]B. C. Garrett and D. G. Truhlar, J. Phys. Chem. **89**, 2204 (1985).
[48]B. C. Garrett, D. W. Schwenke, T. R. Skodje, D. Thirumalai, T. C. Thompson, and D. G. Truhlar, Am. Chem. Soc. Symp.Ser. **263**, 375 (1984).
[49]M. C. Colton and G. C. Schatz, Chem. Phys. Lett. **124**, 256 (1986).
[50]J. M. Bowman, Chem. Phys. Lett. **124**, 260 (1986).
[51]E. Pollak, J. Phys. Chem. **90**, 3619 (1986).
[52]N. C. Blais and D. G. Truhlar, J. Chem. Phys. **88**, 5457 (1988).
[53]G. W. Johnston, B. Katz, K. Tsukiyama, and R. Bersohn, J. Phys. Chem. **91**, 5445 (1987).
[54]I. Schechter, R. Kosloff, and R. D. Levine, Chem. Phys. Lett. **121**, 297 (1985).
[55]I. Schechter and R. D. Levine, Int. J. Chem. Kinet. **18**, 1023 (1986).
[56]I. Schechter, R. Kosloff, and R. D. Levine, J. Phys. Chem. **90**, 1006 (1986).
[57]G. C. Schatz, Chem. Phys. Lett. **108**, 532 (1984).